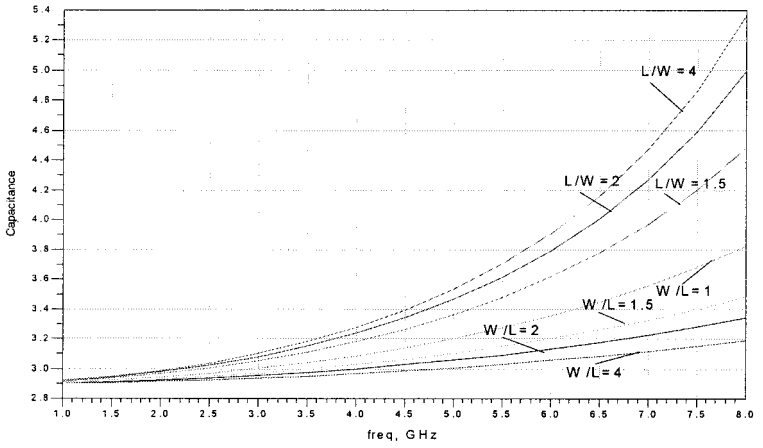

Figure 10 The capacitances of circuit model with different W, L

First of all, the key factor affecting the Q factor of capacitor is tan δ of the thin film. The Q factor can change from 100 to about 700 at 1 GHz when the tan δ turns from 0.01 to 0.001. Unfortunately, for same materials, the tan δ of thin film often changes according to its thickness [8]. So during the design process, a more accurate value of tan δ needs to be known. The design should use a material that has small tan δ.

The height of the substrate can only slightly affect the Q factor of capacitor; at lower frequencies the Q factor is almost the same. At higher frequencies, for example, at 8 GHz, the Q factor can rise about 10% when the height of substrate goes from 50 to 500 μm.

The metal thickness is also an important factor affecting the Q factor of capacitor [9]. When the metal thickness is larger than skin depth, the Q factor remains almost the same. But when the metal thickness is smaller than skin depth, the Q factor drops quickly. From Figure 6, it can be seen that when the metal thickness changes from 2 to 0.2 μm, the Q factor at 1 GHz drops from about 330 to 40 or so. In capacitor production, usually only the bottom metal layer is evaporated, and hence is about 0.5 μm thick [9]; this is much less than the skin depth at the lower frequency. This may be part of the reason that the Q factors of many capacitors are about 50 or so [3].

REFERENCES

1. C. Geng et al., Physically-based RF model for metal–oxide–metal capacitors, Electron Lett 36 (2000), 425–427.
2. C.M. Hung et al., High-Q capacitors implemented in a CMOS process for low-power wireless applications, IEEE Trans Microwave Theory Tech, MTT-46 (1998), 505–511.
3. B. Razavi, CMOS technology characterization for analog and RF design IEEE J Solid-State Circuits SSC-34 (1999), 268–276.
4. H. Samavati, A. Hajimiri, A.R. Shahani, G.N. Nasserbakht, and T.H. Lee, Fractal capacitors, IEEE J Solid-State Circuits SSC-33 (1998), 2035–2041.
5. E. Pettenpaul et al., CAD models of lumped elements on GaAs up to 18 GHz, IEEE Trans Microwave Theory Tech MTT-36 (1988).
6. C.P. Yue et al., A physical model for planar spiral inductors on silicon, IEDM (1996), 155–158.
7. J.N. Burghartz, M. Soyuer, and K.A. Jenkins, Microwave inductors and capacitors in standard multilevel interconnect silicon technology, IEEE Trans Microwave Theory Tech MTT-44 (1996), 100–104.
8. T.K. Lshii, Handbook of microwave technology, Academic Orlando, 1995.
9. R.A. Pucel, Design considerations for monolithic microwave circuits, IEEE Trans Microwave Theory Tech MTT-29 (1981).
10. H. Greenhouse, Design of planar rectangular microelectronic inductors, IEEE Trans PHP, PHP-10 (1974), 101–109.
11. R.K. Hoffmann, Handbook of microwave integrated circuits, Artech House, Norwood, MA, 1987.

BROADBAND EQUIVALENT CIRCUIT MODELS FOR CANONICAL CHIRAL ELEMENTS

B. R. Long and D. H. Werner
Department of Electrical Engineering and Applied Research Laboratory
The Pennsylvania State University
University Park, Pennsylvania 16802

Received 5 February 2002

ABSTRACT: *This article introduces broadband equivalent circuit models for both series-connected and parallel-connected canonical chiral elements. Each connection method results in a different terminal impedance behavior and therefore requires a different equivalent circuit model. These equivalent circuit models have a variety of applications including allowing for convenient analysis of chiral antennas as well as meta-materials composed of passively or actively loaded chiral elements.* © 2002 Wiley Periodicals, Inc. Microwave Opt Technol Lett 34: 181–183, 2002; Published online in Wiley InterScience (www.interscience.wiley.com). DOI 10.1002/mop.10410

Key words: *chiral element; chiral materials; meta-materials; equivalent circuit*

1. INTRODUCTION

Atomic and molecular interactions with optical electromagnetic energy give rise to a wide range of optical phenomena. The most intense interaction generally occurs when the optical wavelength and the dimension of the atomic or molecular units are roughly equivalent. However, atomic and molecular dimensions are too small to support significant interactions at radio and microwave frequencies. Lindman [1] first demonstrated optical activity at microwave frequencies by fashioning an artificial medium (i.e., a meta-material) containing metallic helical inclusions. Two aspects

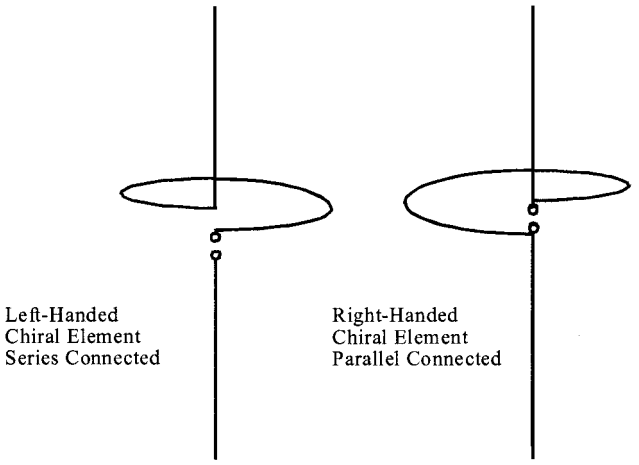

Figure 1 Canonical chiral elements

of helical geometry provide the field cross-coupling basis for optical activity. First, the loops of the helix interact with the magnetic field manifestation of the incident electromagnetic wave. Current induced in the loop is proportional to the time rate of change of the magnetic field vector contained within the circular area bounded by the loop. Second, the linear portion of the helical geometry interacts with that component of the incident electric field having the same orientation. This induced current is proportional to the incident electric field. These helical inclusions are examples of chiral elements [2, 3]. A canonical chiral element is the simplest expression of these two aspects of helix geometry. Both right-handed and left-handed canonical chiral elements are possible, as illustrated in Figure 1.

An external load can be connected to a chiral element in two ways: a parallel connection or a series connection. The parallel connection places the external load across the dipole-loop gap, putting the loop terminals, the dipole terminals, and the load terminals in parallel. The other configuration breaks the connection between the dipole and loop sections at the center gap, reconnecting the loop, the load, and the dipole in a series configuration. Figure 1 shows both connections. The terminal impedance and backscatter behavior of the chiral element is different for each connection method. The objective of this Letter is to develop useful equivalent circuit models for both series-connected and parallel-connected versions of canonical chiral elements.

2. EQUIVALENT CIRCUIT FOR SERIES-CONNECTED CHIRAL ELEMENT

Lumped constant dipole equivalent models often have repetitive circuit topology that mimics the repetitive aspect of dipole overtone responses with one LCR network needed for each response [4]. Chiral element equivalent circuit models can have topologies similar to those employed in dipole circuit models, even though their overtone response fails to follow the familiar odd integer pattern. Figure 2 shows an equivalent circuit for a series connected canonical chiral element. It consists of five parallel-connected series resonant LCR circuits. Each shunt branch provides one reactance zero in the equivalent circuit impedance response at 307, 625, 855, 1880 and 2800 MHz. This circuit was applied to represent a series-connected canonical chiral element with a total wire length of 50 cm, a loop circumference of 25 cm, and a wire radius of 1 mm. Figure 3 shows the resulting frequency response. The solid line represents the terminal impedance of the series-connected chiral element determined by using a method-of-moments

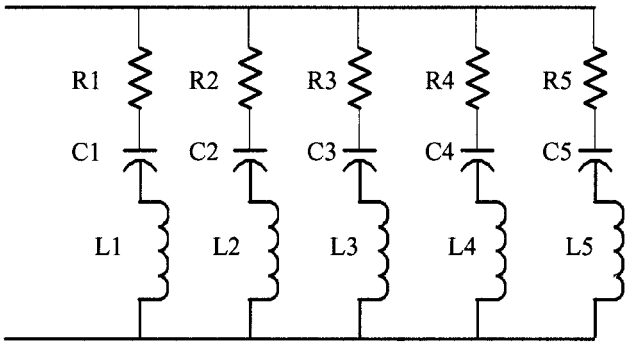

Figure 2 Equivalent circuit for series-connected chiral element

(MoM) approach. The dashed line shows the equivalent circuit terminal impedance for the following component values:

$R1 = 25\Omega$ $R2 = 10\ \Omega$ $R3 = 520\ \Omega$
$C1 = 0.538$ pF $C2 = 0.281$ pF $C3 = 0.099$ pF
L1 = 500 nH L2 = 231 nH L3 = 350 nH

$R4 = 200\ \Omega$ $R5 = 0\ \Omega$
$C4 = 0.159$ pF $C5 = 0.064$ pF
L4 = 45 nH L5 = 50 nH

3. EQUIVALENT CIRCUIT FOR PARALLEL CONNECTED CHIRAL ELEMENT

The same general approach is suitable for the representation of a parallel-connected chiral element by evoking duality, replacing shunt connected series resonant circuits with series-connected parallel resonant circuits as shown in Figure 4. This equivalent circuit has four resonant networks creating impedance poles at 316, 818, 1570, and 2000 MHz. The equivalent circuit component values for this model are

$R1 = 10\text{k}\Omega$ $R2 = 10\ \Omega$ $R3 = 520\ \Omega$ $R4 = 200\ \Omega$
$C1 = 0.538$ pF $C2 = 0.281$ pF $C3 = 0.099$ pF $C4 = 0.159$ pF
L1 = 500 nH L2 = 231 nH L3 = 350 nH L4 = 45 nH

Figure 5 shows the impedance as a function of frequency for a parallel-connected canonical chiral element with the same dimen-

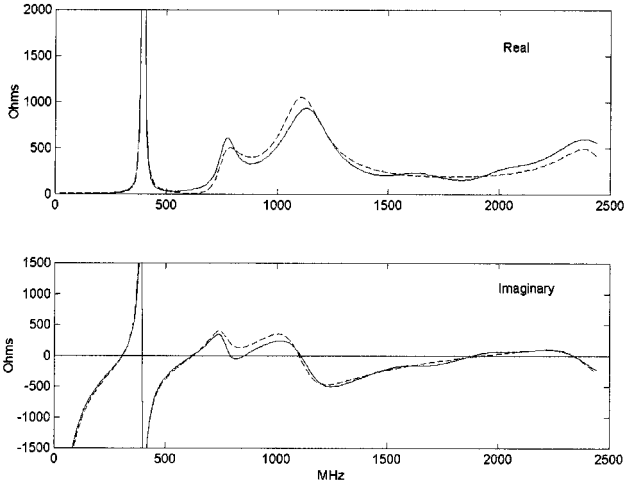

Figure 3 Impedance of series-connected chiral element and five-branch equivalent circuit

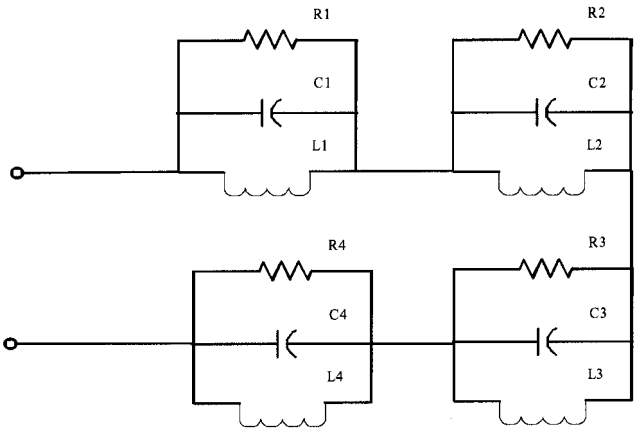

Figure 4 Equivalent circuit for parallel-connected chiral element with four impedance poles

sions and geometry as in the previous case. The solid line is the impedance of the chiral element determined by a MoM analysis and the dashed line is the terminal impedance of the equivalent circuit network.

Removing the circuitry responsible for the 1570-MHz impedance pole gives the response shown in Figure 6. In this case the reduced component count equivalent circuit still has fairly good correspondence with the chiral element impedance. After a slight readjustment, the impedance poles of the reduced complexity equivalent circuit fall at 316, 808, and 2000 MHz. The dashed line represents the impedance of the equivalent circuit network as before. The circuit component values in this case are

$R1 = 10\text{k}\Omega$ $R2 = 900$ $R3 = 550\ \Omega$
$C1 = 1.26$ pF $C2 = 1.29$ pF $C3 = 0.792$ pF
L1 = 200 nH L2 = 30 nH L3 = 8 nH

4. CONCLUSIONS

Several useful broadband equivalent circuit models for chiral elements have been presented and discussed in this article. In particular, equivalent circuit models were developed for both series-connected and parallel-connected versions of the standard canonical loop–dipole representation of a helix. The parameters of these equivalent circuit models were adjusted to yield the best possible fit to the actual frequency response curves calculated by a rigorous numerical analysis procedure based on the method of moments. These equivalent circuit models may be used to aid in the design of chiral antennas as well as electromagnetic meta-materials composed of chiral elements with passive or active loads.

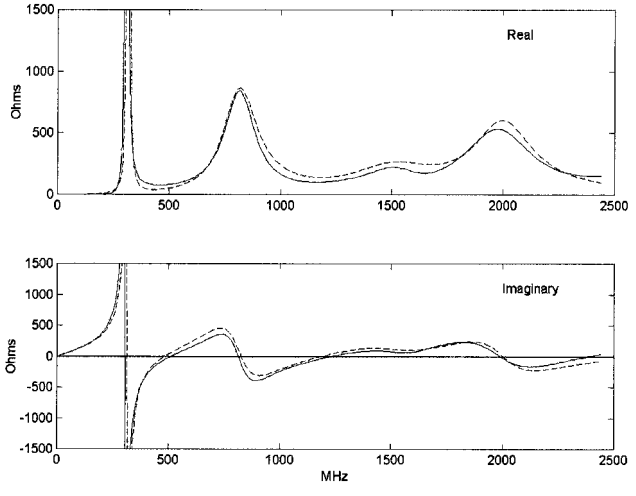

Figure 5 Impedance of parallel-connected chiral element and four-pole equivalent circuit

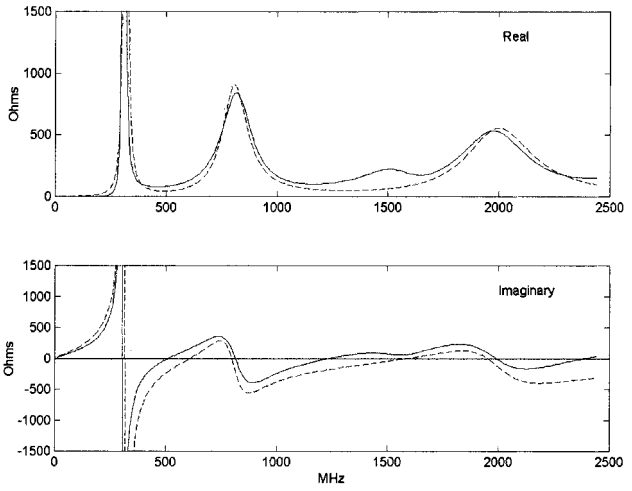

Figure 6 Impedance of parallel-connected chiral element and three-pole equivalent circuit

REFERENCES

1. K.F. Lindman, Om en geron att isotropt system av spiralformiga resonatorer alstrad rotationspolarisation av de elektromagnetiska vagorna, Oevers Fin Vetensk Soc Foerh 57 (1914-1915), 1–32.
2. I.V. Lindell, A.H. Sihvola, S.A. Tretyakov, A.J. Viitanen, Electromagnetic waves in chiral and bi-isotropic media, Artech House, Boston, 1994.
3. D.L. Jaggard, A.R. Mickelson, C.H. Papas, On electromagnetic waves in chiral media, Appl Phys 18 (1979), 211–216.
4. B.R. Long, P.L. Werner, D.H. Werner, Genetic algorithm optimization of dipole equivalent circuit models, Microwave Opt Technol Lett 27 (2001), 259–261.

COMPACT DUAL-FREQUENCY SHORTED RHOMBIC MICROSTRIP ANTENNA WITH A PAIR OF SLITS

Yi-Fang Lin, Chin-Chun Kuo, and Hua-Ming Chen
Department of Physics
National Kaohsiung University of Applied Sciences
Kaohsiung 807, Taiwan

Received 10 January 2002

ABSTRACT: *By using a pair of shorting pins, the dual-frequency operation of a single-feed rhombic microstrip antenna with a pair of slits is presented. This shorted dual-frequency microstrip antenna can result in a much reduced antenna size, and provide a tunable frequency ratio of ~1.26–2.33 for the two operating frequencies by varying the inset slit length. Simulated results with the use of the software also have been conducted to study the characteristics of these antennas. Details of the pro-*